

Collapse of the Zeeman structure of the hydrogen atom in an external electric field

D. A. Sadovskii,¹ B. I. Zhilinskiĭ,¹ and L. Michel²

¹Université du Littoral, Boîte Postale 5526, F59379 Dunkerque Cedex 1, France

²Institut des Hautes Etudes Scientifiques, Bures-sur-Yvette, F91440, France

(Received 26 September 1995)

We analyze the transition from a Zeeman to a Stark structure of a weakly split Rydberg n multiplet of the H atom in parallel magnetic and electric fields. The use of classical mechanics, topology, and group theory provides a detailed description of the modifications of dynamics due to the variation of the electric field. We focus on the point where the collapse of the Zeeman structure occurs, give the sequence of classical bifurcations responsible for the transition between different dynamic regimes, and compare it to the quantum energy-level structure. [S1050-2947(96)10906-9]

PACS number(s): 32.60.+i, 03.20.+i

Rydberg atoms in parallel magnetic and electric fields have been studied extensively both theoretically and experimentally during the last decade. In particular, many studies have focused on the situation where the fields are (relatively) weak and the dynamics can be analyzed in terms of additional approximate integrals of motion [1–8]. We use a similar idea to analyze several dynamic regimes that exist for different strength of the electric (F) and magnetic (G) fields. These regimes clearly manifest themselves in the energy level pattern in Fig. 1. At very weak electric field, where most of the studies [1–8] have been done, we have a structure characteristic of the second-order Zeeman effect (see Fig. 2). When F increases this structure quickly disappears. Instead we observe regular “resonance” structures at certain values of F (see Fig. 1). This culminates in an almost complete collapse of the internal structure. Surprisingly, and contrary to the $F \sim 0$ case the dynamics near this collapse has not, to our knowledge, been analyzed. Furthermore, exist-

ence of collapsed levels with different projections of the orbital momentum m can be used in the experiment to selectively produce states with any possible m using adiabatic change of field parameters [9]. In this paper we give a detailed analysis of the collapse region.

Neglecting the spin effects the Hamiltonian for the hydrogen atom in constant parallel magnetic γ and electric f fields (along the z axis) has the form (in atomic units)

$$H = \frac{p^2}{2} - \frac{1}{r} + \frac{\gamma}{2}L_z + \frac{\gamma^2}{8}(x^2 + y^2) - fz, \quad (1)$$

with γ and f in units of 2.35×10^5 T and 5.14×10^9 V/cm. We restrict ourselves to the low field case where the splitting of an n shell caused by both fields is small compared to the splitting between neighboring n shells (see Fig. 3). As is well known, in the absence of electric field low- m submanifolds of the n shell show the characteristic pattern of the second-order Zeeman effect. When the electric field effect is of the

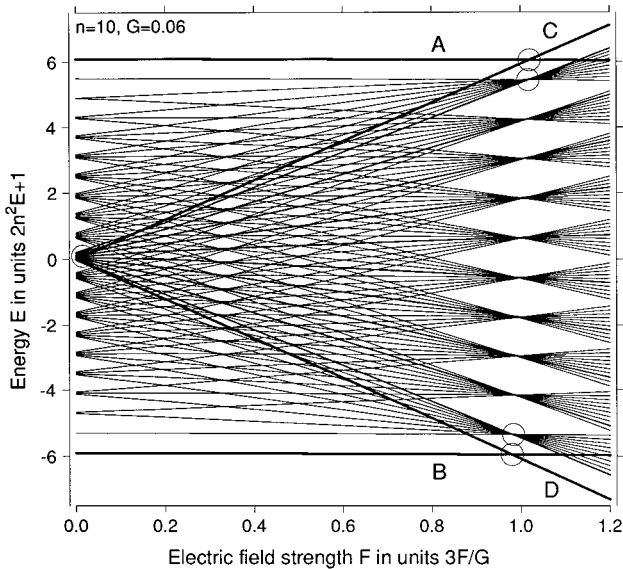


FIG. 1. Collapse of the Zeeman structure for the magnetic field $G=0.06$ due to the increasing electric field. Quantum levels are calculated for the $n=10$ multiplet of the hydrogen atom. Electric field strength is given in units $F_0=G/3$ [see Eq. (3)].

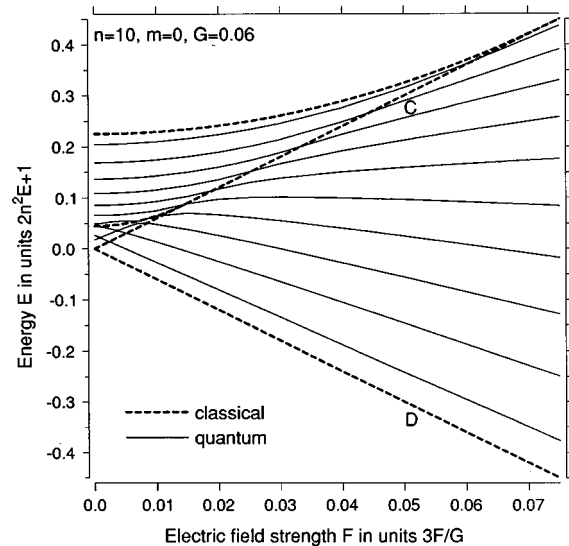


FIG. 2. Deformation of the quantum Zeeman effect structure of the $n=10, m=0$ multiplet of the hydrogen atom. Dashed lines show the energy in stationary points of classical Hamiltonian restricted on $\mu=0$.

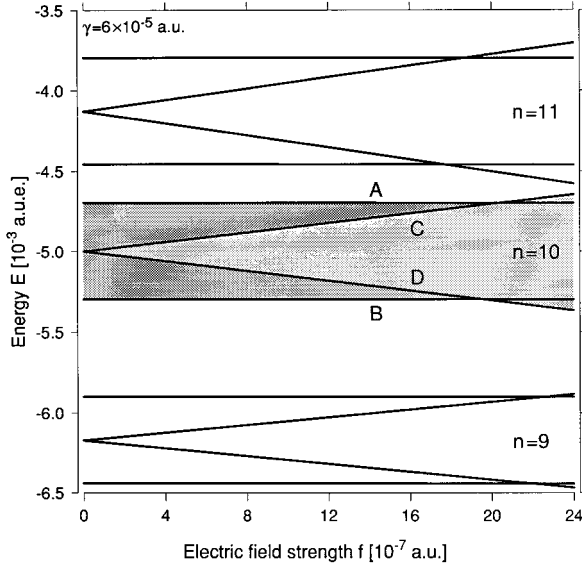


FIG. 3. Neighboring Rydberg multiplets $n=9,10,11$ of the hydrogen atom. a.u.e. denotes atomic unit of energy.

same order as the quadratic Zeeman effect (see Fig. 2), this pattern disappears and turns into a Stark structure for each m submanifold [4,6]. Much less attention has been paid to the region where the Stark splitting of the n shell ($\propto 3fn^2$) is of the same order as the n shell splitting due to magnetic field ($\propto \gamma n$) (Fig. 1, region near $3F/G=1$), in other words when

$$f_0 = \gamma/3n. \quad (2)$$

Equation (2) gives the collapse condition for shell n . To ensure that this collapse happens when the n -shell splitting remains small compared to the gap between n shells we take $\gamma < 1/n^4$. Under this assumption we can study an isolated n shell and can use scaling

$$F = fn^4, \quad G = \gamma n^3, \quad \tilde{E}_n = 2n^2 E_n + 1, \quad (3)$$

to remove n from the effective n -shell Hamiltonian [Eq. (7) below]. This transforms the initial collapse condition (2) into $F_0 = G/3$.

Our purpose is to study the dynamics under the variation of the electric field f in the neighborhood of its critical value f_0 . The natural parameter for this study is $\delta = 3F/G - 1 = 3fn/\gamma - 1$.

The analysis is based on the transformation of the initial Hamiltonian (1) into an effective one for an individual n shell. This can be done either by quantum or by classical perturbation theory [6–8].

An effective n -shell Hamiltonian can be expressed in terms of angular momentum \mathbf{L} and Runge-Lenz vector $\mathbf{A} = \mathbf{p} \times \mathbf{L} - \mathbf{r}/r$, or, alternatively, in terms of their linear combinations $\mathbf{J}_1 = (\mathbf{L} + \mathbf{A})/2$ and $\mathbf{J}_2 = (\mathbf{L} - \mathbf{A})/2$. For the linear Stark-Zeeman effect in parallel fields the effective Hamiltonian is

$$H = \frac{1}{2n^2} (-1 + \gamma n^2 L_z + 3fn^3 A_z). \quad (4a)$$

If we impose the relation between field strengths (2) this Hamiltonian becomes

$$H = \frac{1}{2n^2} [-1 + 3f_0 n^3 (J_1)_z]. \quad (4b)$$

The n^2 energy levels in the n shell described by (4b) form n -fold degenerate groups. The levels in each group are labeled by the same value of $(J_1)_z$ and by different values of $(J_2)_z$. Figure 1 shows how the Zeeman structure of the n shell at $f=0$ transforms into this highly degenerate structure at $f=f_0$ ($F=G/3$). We call this effect the collapse of the Zeeman structure caused by electric field. To describe the fine structure of each $(J_1)_z$ manifold of states the second-order effects should be taken into account.

To develop the effective n -shell Hamiltonian to higher orders we consider n as an integral of motion and use the perturbation theory to reduce the initial problem (1) to two degrees of freedom. Naturally, the pair (L_z, ϕ_{L_z}) describes one of these degrees; the other degree can be described by A_z and ϕ_{A_z} [7]. Of course, for Hamiltonian (1) L_z is strictly conserved and the n -shell Hamiltonian does not depend on ϕ_{L_z} . However, to study the collapse we should consider the energy-level structure of the n shell as a whole, and therefore, we should keep L_z as a dynamical variable. Hence our n -shell Hamiltonian is a function of dynamical variables (L_z, A_z, ϕ_{A_z}) and parameters (n, f, γ) .

The classical phase space Σ for an effective n -shell Hamiltonian is a four-dimensional space with topology $S_2 \times S_2$ (S_2 is a 2D sphere). Its parametrization can be done either using \mathbf{L}, \mathbf{A} variables with $\mathbf{L}^2 + \mathbf{A}^2 = n^2$, and $\mathbf{L} \cdot \mathbf{A} = 0$, or using $\mathbf{J}_1, \mathbf{J}_2$ variables with $\mathbf{J}_1^2 = \mathbf{J}_2^2 = n^2/4$. (In the classical limit n is sufficiently large and $n^2 \approx n^2 - 1$.)

For the qualitative analysis of the n -shell dynamics special variables

$$\nu = A_z/n, \quad \mu = L_z/n, \quad \xi = (L^2 - A^2)/n^2. \quad (5)$$

are the most useful. This choice of variables (5) is based on group theory and, in particular, on invariant theory. In fact, (ν, μ, ξ) form the set of invariant polynomials (the so-called integrity basis) that is used both to label the points of the phase space and to expand the Hamilton function [10,11]. Furthermore, the proper scaling in (5) and (3) results in equations that do not depend on n .

The symmetry group \mathcal{G} of the problem is made up of the rotations r_θ and operations (Ts_ϕ) . r_θ are rotations around the ‘‘vertical’’ axis oz , the common direction of the electric and magnetic field; they form the group C_∞ . Each operation (Ts_ϕ) is a product of time reversal T and reflection s_ϕ through a vertical plane that contains oz and has azimuth ϕ . We emphasize that neither T nor s_ϕ is separately a symmetry of the problem. We verify that $(Ts_\phi)^2 = 1$, $(Ts_\phi)r_\theta(Ts_\phi) = r_{-\theta} = r_\theta^{-1}$, and $r_\theta(Ts_\phi)(r_\theta)^{-1} = Ts_{\phi+\theta}$. So \mathcal{G} is isomorphic (but not identical) to the group $C_{\infty v}$ and the (Ts_ϕ) 's form one conjugacy class of \mathcal{G} .

Consecutive steps in the qualitative analysis of an effective Hamiltonian under the presence of the symmetry group [11] includes the study of the action of the symmetry group on the classical phase space, construction of the space of

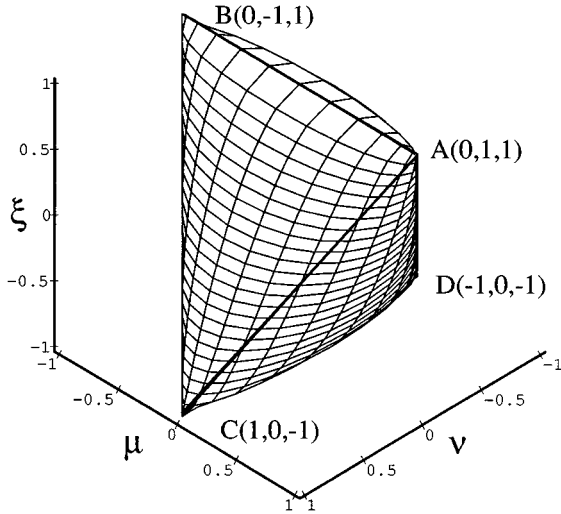


FIG. 4. The space of orbits of the symmetry group of the Rydberg electron in the presence of parallel electric and magnetic fields in the n -shell approximation.

orbits (orbifold), and the analysis of the system of stationary points (orbits) of the Hamilton function using the topological and group theoretical information about the phase space. To study the action of \mathcal{G} on Σ we just need the following facts: \mathbf{L} and \mathbf{A} are, respectively, axial and polar vectors, and T reverses \mathbf{L} . This allows us to find all orbits of the action of the group \mathcal{G} on Σ . According to the general theory of invariants, different orbits can be distinguished by three (algebraically independent) invariants of \mathcal{G} and every smooth \mathcal{G} -invariant function on Σ is a smooth function of these invariants. We have chosen ν, μ, ξ in (5) as these basic invariants. The possible range of variation of ν, μ, ξ is given by a \mathcal{G} -invariant function $\sigma^2 = [(\mathbf{L} \times \mathbf{A}) \cdot \mathbf{n}]^2$, with \mathbf{n} the unit vector of oz . It is a polynomial of ν, μ, ξ and it gives a representation of the space of orbits \mathcal{O} (see Fig. 4):

$$\mathcal{O}: -1 \leq \xi \leq 1,$$

$$4\sigma^2 = 1 - \xi^2 - 2(1 - \xi)\mu^2 - 2(1 + \xi)\nu^2 \geq 0. \quad (6)$$

Every orbit is represented by a point of \mathcal{O} [12]. There are three strata. They contain, respectively, (i) four fixed points A, B, C, D , with \mathcal{G} the stabilizer; these four points are also called four critical orbits since they are extrema of any \mathcal{G} -invariant function on Σ [10]; their coordinates (ν, μ, ξ) are given in Fig. 4; (ii) a two-parameter family of circles S_1 (orbits of C_∞) whose points have $\{1, Ts_\phi\}$ as stabilizers; these orbits belong to the boundary of \mathcal{O} given by the equation $\sigma = 0$; we remark that this boundary contains the edges of the tetrahedron with vertices A, B, C, D ; (iii) a three-parameter family of generic orbits made of a pair of circles ($=2S_1$) with trivial stabilizer 1 (internal points of the orbifold).

The Hamilton function can be expressed as a polynomial $H = H(\nu, \mu, \xi)$ of invariant polynomials ν, μ, ξ . Up to quadratic in F and G terms the scaled energy \tilde{E} has the form

$$\begin{aligned} \tilde{E} = & G\mu + 3F\nu - \frac{1}{4}G^2\xi + \frac{1}{8}(9F^2 + G^2)\mu^2 \\ & + \frac{1}{8}(3F^2 - 5G^2)\nu^2 + \frac{1}{8}(3G^2 - 17F^2). \end{aligned} \quad (7)$$

To qualitatively characterize classical and quantum dynamics we find the system of stationary points (manifolds) of the energy function on the phase space. Group theory asserts that four points A, B, C, D (critical orbits) must be stationary for any smooth function defined over the phase space [10]. Energy values (7) at these points are shown in Figs. 1 and 3. Morse inequalities confirm that the simplest Morse-type functions possessing stationary points only on the four critical orbits really exist on Σ and have one minimum, one maximum, and two saddle points. For more complicated functions any other stationary points can be found by looking for those energy sections of the orbifold that correspond to the modification of the topology of the energy section.

Simple geometrical analysis shows that in the linear (in F and G) approximation for $F < F_0$ the energy function is of the simplest type with a minimum in B , a maximum in A , and two saddle points in C and D . For $F > F_0$ the energy function is again of the simplest type with a minimum in D , maximum in C , and two saddle points in A and B . Sudden transition from one simple type of energy function to another in the linear model occurs due to the formation of the degenerate stationary manifold at $F = F_0$ corresponding to Hamiltonian (4b). In the linear model the energy surface touches the orbifold through the whole interval $[C, A]$ or $[B, D]$. Introduction of the F^2 and G^2 terms into the energy function removes this degeneracy. The energy surface (7) is the second-order surface in ξ, μ, ν variables. It can touch orbifold \mathcal{O} at some isolated points on the $\sigma = 0$ surface, which are different from the critical orbits A, B, C, D . If this happens, additional stationary orbits are present. A detailed analysis of a system of stationary points as a function of F near the collapse value F_0 shows how the transformation from the Zeeman-type energy function (with only four stationary critical orbits having minimum and maximum in B and A) to the Stark-type energy function (with only four stationary critical orbits having minimum and maximum in D and C) occurs. Two sequences of bifurcations are present with two bifurcations in each sequence. As F increases, one sequence begins with a bifurcation at point B , which creates a new stationary S_1 orbit of \tilde{E} on Σ . The corresponding point on the surface of the orbifold moves from B to D and disappears at D after the second bifurcation. Another sequence of bifurcations proceeds in a similar way with two bifurcations at C and A and the additional stationary orbit moving from C to A .

Positions of all stationary orbits can be found by solving the Hamiltonian equations on Σ . An alternative way is to use the geometrical representation of the orbifold and of the energy surface. To find noncritical stationary orbits we find points where the energy surface touches the orbifold. In other words we find points where the normal vector to the $\sigma = 0$ surface and the normal vector to the energy surface $\mathbf{k} = (k_\nu, k_\mu, k_\xi)$ are collinear. This geometric view gives us extremely simple conditions for bifurcations at points A, B, C, D :

$$A: 4k_\xi k_\mu = k_\nu^2 - k_\mu^2; \quad \delta_A \approx -G^2/8 - G^3/16, \quad (8a)$$

$$C: 4k_{\xi}k_{\nu} = k_{\nu}^2 - k_{\mu}^2; \quad \delta_C \approx 2G/3 + G^2/72, \quad (8b)$$

$$B: 4k_{\xi}k_{\mu} = k_{\mu}^2 - k_{\nu}^2; \quad \delta_B \approx -G^2/8 + G^3/16, \quad (8c)$$

$$D: 4k_{\xi}k_{\nu} = k_{\mu}^2 - k_{\nu}^2; \quad \delta_D \approx -2G/3 + G^2/72. \quad (8d)$$

When δ varies between δ_A and δ_C an additional stationary orbit exists on the surface of the orbifold and moves from point A to point C. Similarly for δ between δ_D and δ_B another additional stationary orbit moves from D to B. The energies of all stationary orbits near the bifurcation points and the quantum energy levels are shown in Fig. 5.

A simple quantum mechanical interpretation of the effect of the transformation of the Zeeman-type structure into the Stark-type one can be done by looking at the two extremal states (with minimal and maximal energy) of the same n multiplet (Fig. 5). We can characterize each extremal state by two average values, $\langle L_z \rangle$ and $\langle A_z \rangle$. From the positions of stationary points on the orbifold it follows immediately that for the state with maximal energy $\langle L_z \rangle \approx n$ for $\delta < \delta_A$ and $\langle L_z \rangle \approx 0$ for $\delta > \delta_C$, whereas $\langle L_z \rangle$ varies almost linearly with δ for $\delta_A < \delta < \delta_C$. For the same state $\langle A_z \rangle \approx 0$ for $\delta < \delta_A$ and $\langle A_z \rangle \approx n$ for $\delta > \delta_C$, whereas $\langle A_z \rangle$ varies almost linearly with δ for $\delta_A < \delta < \delta_C$.

We conclude that important qualitative modifications of dynamics take place in the collapse region. This suggests new experimental investigations that can use the detailed information on many energy-level crossings in the collapse

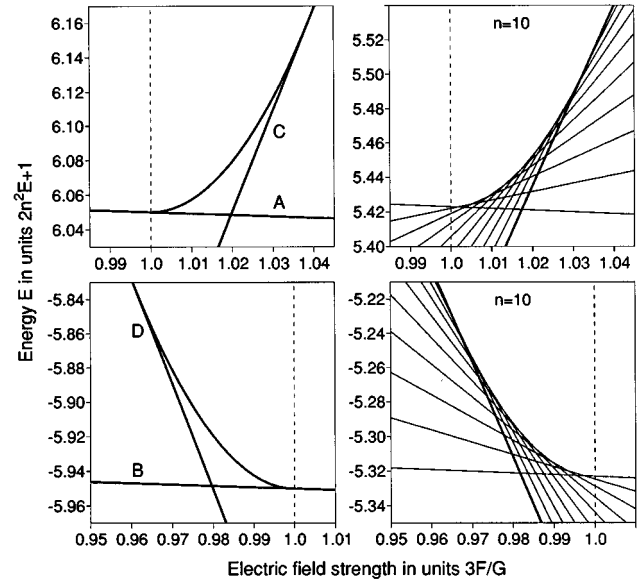


FIG. 5. Bifurcation diagram near the collapse region. Classical (left) vs quantum (right) representation.

region to obtain quantum states with desired properties by fine tuning the field parameters. The present paper also demonstrates the powerful geometrical and group theoretical technique based on the orbifold representation.

-
- [1] P. Cacciani, E. Luc-Koenig, J. Pinard, C. Thomas, and S. Liberman, *J. Phys. B* **21**, 3473 (1988); **21**, 3499 (1988); **21**, 3523 (1988); *Phys. Rev. A* **40**, 3026 (1989); *J. Phys. B* **25**, 1991 (1992).
- [2] A. König, J. Neukammer, K. Vietzke, M. Kohl, H.-J. Grabka, H. Hieronymus, and H. Rinneberg, *Phys. Rev. A* **38**, 547 (1988).
- [3] T. van der Veldt, W. Vassen, and W. Hogervorst, *J. Phys. B* **26**, 1945 (1993).
- [4] P. A. Braun and E. A. Solov'ev, *Zh. Éksp. Teor. Fiz.* **86**, 68 (1984) [*Sov. Phys. JETP* **59**, 38 (1984)].
- [5] P. A. Braun, *Rev. Mod. Phys.* **65**, 115 (1993).
- [6] D. Delande and J. C. Gay, *Phys. Rev. Lett.* **66**, 3237 (1991).
- [7] D. Farrelly, T. Uzer, P. E. Raines, J. P. Skelton, and J. Milligan, *Phys. Rev. A* **45**, 4738 (1992).
- [8] E. A. Solov'ev, *Pis'ma Zh. Éksp. Teor. Fiz.* **82**, 1762 (1981) [*JETP Lett.* **34**, 265 (1981)]; D. R. Herrick, *Phys. Rev. A* **26**, 323 (1982).
- [9] D. Delande and J. C. Gay, *Europhys. Lett.* **5**, 303 (1988); R. G. Hulet and D. Kleppner, *Phys. Rev. Lett.* **51**, 1430 (1983).
- [10] L. Michel, *Rev. Mod. Phys.* **52**, 617 (1980).
- [11] D. A. Sadovskii and B. I. Zhilinskii, *Phys. Rev. A* **47**, 2653 (1993).
- [12] We recall that the type of orbit that appears in a group action is characterized by the conjugacy class of the stabilizers of the points of the orbit. The union of all orbits of the same type is called a stratum [10].